ACS OMEGA

http://pubs.acs.org/journal/acsodf

Article

Highly Efficient, Environmentally Friendly Lignin-Based Flame Retardant Used in Epoxy Resin

Peng Dai,[⊥] Mengke Liang,[⊥] Xiaofeng Ma, Yanlong Luo, Ming He, Xiaoli Gu, Qun Gu, Imtiaz Hussain, and Zhenyang Luo*

Cite This: *ACS Omega* 2020, 5, 32084−32093

Read Online

ACCESS | Metrics & More | Article Recommendations | Supporting Information

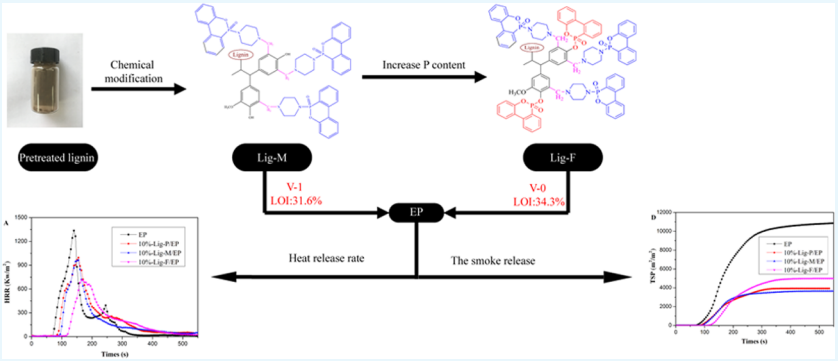

ABSTRACT: We prepared novel flame retardants with concurrent excellent smoke-suppression properties based on lignin biomass modified by functional groups containing N and P. Each lignin-based flame retardant (Lig) was quantitatively added to a fixed amount of epoxy resin (EP), to make a Lig/EP composite. The best flame retardancy was achieved by a Lig-F/EP composite with elevated P content, achieving a V-0 rating of the UL-94 test and exhibiting excellent smoke suppression, with substantial reduction of total heat release and smoke production (by 46.6 and 53%, respectively). In this work, we characterized the flame retardants and the retardant/EP composites, evaluated their performances, and proposed the mechanisms of flame retardancy and smoke suppression. The charring layer of the combustion residual was analyzed using SEM and Raman spectroscopy to support the proposed mechanisms. Our work provides a feasible method for lignin modification and applications of new lignin-based flame retardants.

1. INTRODUCTION

Polymer materials are ubiquitous in our daily lives due to their excellent mechanical and physicochemical properties.[1−3] However, most of these materials are highly flammable and produce a large amount of heat and smoke during combustion, limiting their applications when fire resistance is required.[4] Therefore, flame retardants and smoke suppressants have become an emerging focus of research.[5,6] Halogen-[7] and petroleum-based[8] flame retardants have been developed in the past, but their development raised concerns about their negative environmental impacts and consumption of fossil-based resources. Inevitably, flame retardants based on green and renewable biomass resources are receiving increased attention; yet, recent research has plenty of room for improvement. Currently, flame retardants based on modification of biomass resources have been successfully applied to polymer materials with reasonable effectiveness, such as phytic acid,[9,10] starch,[11] castor oil,[12] bamboo fiber,[13] cardanol,[14] cellulose,[15,16] and lignin.[17,18] Among these, lignin has great potential due to its abundance in nature and because it is widely found in supporting tissues of plants such as wood and bark. With a high carbon content and multireactive functional groups, lignin has become a promising and environmentally friendly resource for flame retardants. Its thermal properties have been studied extensively.[19] It is reported that lignin initiates thermal degradation in a wide temperature range above 150 °C and forms a thermally stable product (char) at 700 °C.[20,21] The charring layer prevents spreading of oxygen and transfer of heat, thereby inhibiting further combustion.[22−24] Although a large amount of lignin was directly burned as an energy source in the past, research on utilizing lignin in flame retardants has started to increase recently.[25] Two types of preparations for lignin-based flame retardants are commonly reported. The first type is physical blending,[26,27] in which lignin is added directly into the polymers as a synergist of other traditional flame retardants, such as APP, melamine,

Received: October 22, 2020
Accepted: November 26, 2020
Published: December 4, 2020

https://dx.doi.org/10.1021/acsomega.0c05146
ACS Omega 2020, 5, 32084−32093

and $Al(OH)_3$. A disadvantage of this type of method is uneven multicomponent mixing, which has a negative impact on flame retardancy. The second type comprises methods of chemical modification,[28−30] in which desired functional groups are grafted onto lignin by chemical reactions. Chemically modified lignin-based flame retardants containing nitrogen and phosphorus with promising performances have been reported.[31] However, lignin-based flame retardants prepared by the conventional modification route have rarely achieved the rating of V-0 in the UL-94 flammability standards[32] and little attention was paid to smoke suppression.[33] Although reports show that epoxy resins containing lignin model compounds can achieve reasonable flame-retardant and smoke-suppression effects,[34,35] these methods are not based on natural lignin biomass. As an alternative, our work aims to develop effective flame retardants with superior smoke-suppression properties using modified pristine lignin, for polymer materials.

We used two components with excellent flame retardancy,[36,37] piperazine (PA) and 9,10-dihydro-9-oxa-10-phosphaphenanthrene-10-oxide (DOPO), to prepare the intermediates (PA−DOPO), as described in Scheme S1 in the Supporting Information. By the Mannich reaction, we grafted PA−DOPO onto pretreated lignin (Lig-P; see Scheme S2 in the Supporting Information), which was then chemically bonded to epoxy resin to form a Lig-M/EP composite. The UL-94 test shows that the Lig-M/EP composite reaches a rating of V-1. Further, we grafted DOPO onto Lig-M via the Atherton−Todd reaction between DOPO and phenol groups, to obtain Lig-F, which contains a higher content of element P.[38] The Lig-F/EP composite achieves a UL-94 rating of V-0. Both Lig-M/EP and Lig-F/EP exhibit excellent smoke-suppression properties (see Section 3.3). The structural advantages and high phosphorus content of our lignin-based flame retardants have shown much improved flame-retardant and smoke-suppression performances.

2. RESULTS AND DISCUSSION

2.1. Characterization of Modified Lignins. FT-IR spectra of Lig-P, Lig-M, and Lig-F are shown in Figure 1.

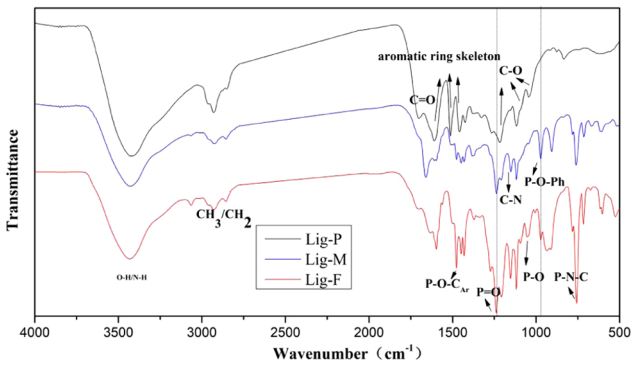

Figure 1. Infrared spectra of Lig-P, Lig-M, and Lig-F.

For Lig-P, the stretching vibrations for OH groups appear at 3429 cm^{-1} as a relatively broad band, while the C−H stretching vibrations for CH−, CH_2−, and CH_3− are at 2930 cm^{-1}. The peaks for the carbonyl group (C═O) appear at 1700 cm^{-1}, characteristic peaks of the aromatic rings are at 1460, 1600, and 1510 cm^{-1}, respectively, and the C−O stretching vibrations for primary alcohol are at 1020 cm^{-1}; all of the above peaks are in line with FTIR absorption peaks reported for pristine lignin.[31]

Lig-M and Lig-F show the C−H stretching of the grafted-CH_2 group at 3067 cm^{-1}, which is absent on the IR spectra of Lig-P. The peak for the C−N bond appears at 1153 cm^{-1}, and that for the P−N bond appears at 762 cm^{-1}. The P═O stretching occurs at 1235 cm^{-1}. The absorption peaks at 1055 and 1276 cm^{-1} are attributed to the stretching vibrations of P−O and P−O−C_{Ar}, respectively. The absorption band at 974 cm^{-1} corresponds to the characteristic absorption peak of the P−O−Ph benzene ring skeleton. These results indicate that the intermediate, PA−DOPO, has been grafted onto the lignin successfully. Furthermore, for Lig-F, the unique peak at 1275 cm^{-1} is the characteristic absorption peak for O−P after the phenol group is connected to DOPO.[39] These results show that nitrogen and phosphorus have been successfully grafted onto our lignin-based intumescent flame retardants.

Elemental analysis was performed to determine the contents of C, H, and N in the modified lignins. As shown in Table 1,

Table 1. Contents of C, H, and N in Modified Lignins Based on Elemental Analysis

	carbon (wt %)	hydrogen (wt %)	nitrogen (wt %)
Lig-P	51.20	5.98	1.46
Lig-M	72.48	5.76	5.42
Lig-F	62.44	5.25	3.09

Lig-P has a low content of residual nitrogen (1.46%) due to the enzymatic hydrolysis process. After PA−DOPO was grafted onto Lig-P, the nitrogen content of Lig-M increased to 5.42%. After further DOPO grafting onto Lig-M, the nitrogen content of Lig-F became 3.09%, which was a relative decrease due to the introduction of P content.

XPS is used to determine the elemental composition of C, O, N, and P in lignins. As shown in Figure 2, N and P were not

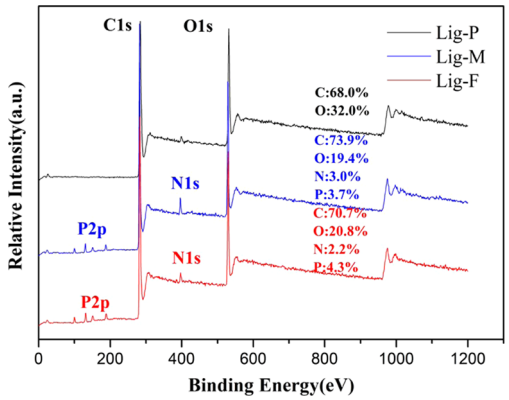

Figure 2. XPS spectra along with the elemental composition of Lig-P, Lig-M, and Lig-F.

found in Lig-P, while C and O were found to be 68.0 and 32.0 wt %, respectively. For Lig-M, N (3.0 wt %) and P (3.7 wt %) were detected in addition to C and O, indicating successful grafting of PA and DOPO onto Lig-P. For Lig-F, further introduction of DOPO increased the P content (4.3 wt %), while the N content decreased (2.2 wt %) relatively. These results are consistent with IR and elemental analyses, confirming the successful introduction of N and P into the lignins via the intermediates PA−DOPO and DOPO.

https://dx.doi.org/10.1021/acsomega.0c05146
ACS Omega 2020, 5, 32084−32093

Introduction of DOPO increases the P content, which leads to an optimized fire-retardant effect.

2.2. Thermal Stability. TGA tests were used to determine the thermal stability of Lig-P, Lig-M, and Lig-F. As shown in Figure 3 and Table 2, Lig-P starts to degrade at 163 °C (T_i, the temperature at which 5 wt % mass loss occurs), with maximal weight loss at about 407 °C (T_{max}, the temperatures at which maximum mass loss occurs); at 800 °C, the residue became 41.0 wt % of the original mass. These values are consistent with reports in the literature.[31]

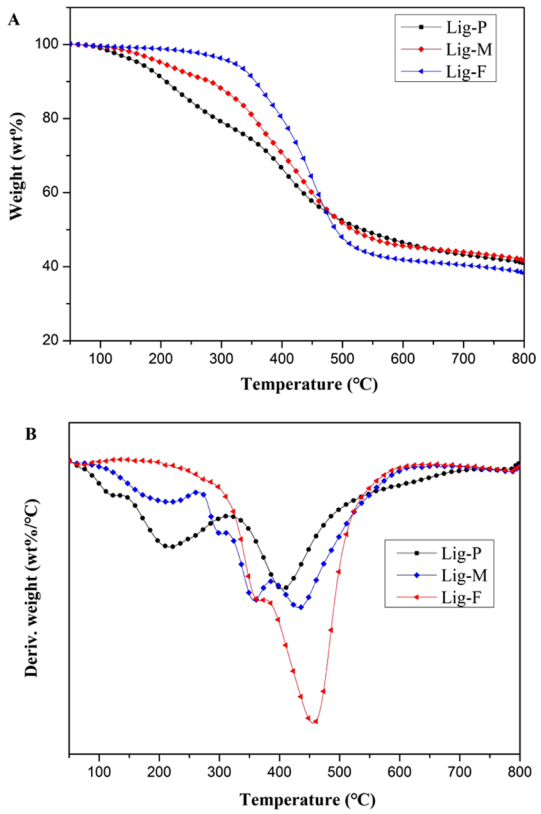

Figure 3. TGA (A) and DTG (B) curves for Lig-P, Lig-M, and Lig-F under nitrogen.

Table 2. Initial Degradation Temperature (T_i), Maximum Weight Loss Temperature (T_{max}), and Carbon Residue (Char) of Lignin and Modified Lignins

	T_i (°C)	T_{max} (°C)	char (%, 800 °C)
Lig-P	163	407	41.0
Lig-M	202	433	41.6
Lig-F	320	455	38.2

The significant increase of T_i and T_{max} confirms the dehydration action of phosphoric acid derivatives in PA–DOPO.[21] T_i and T_{max} of Lig-F are 320 and 455 °C, respectively, much higher than those of Lig-M (202 and 433 °C, respectively). This shows that Lig-F has better thermal stability and flame retardancy than Lig-M. However, Lig-M seems to have slightly better carbonization ability, and the carbon residue is 41.6 wt % of the original mass, as compared to 38.2 wt % for Lig-F.

Figure 4 shows the thermal degradation of EP and Lig/EP composites, and Table 3 shows the data in detail. Compared with the blank epoxy resin, after adding 10 wt % of Lig-P, Lig-M, and Lig-F, T_i of the correspondent composites decreased from 384 to 383, 372, and 354 °C, respectively, and their carbon residue values increased from 14.8 to 16.5, 18.2, and 20.6%, respectively. Adding 10 wt % of Lig-F led to the maximum decrease in T_i and the maximum increase of the carbon residue. As shown by the DTG curve (Figure 4B1), compared to the T_{max} of EP, the T_{max} of 10% Lig-P/EP increased by 3 °C, while the T_{max} values of 10% Lig-M/EP and 10% Lig-F/EP decreased by 7 and 30 °C, respectively. The results shown in Figure 4A2,B2 indicate that, with the increase of the Lig-F concentration in epoxy resin, there is a decrease in both T_i and T_{max}, and an increase in the amount of carbon residue. This is because earlier mass loss promotes earlier carbonization, preventing further combustion.[40,41] This is a result of the excellent performance of Lig-F in flame retardancy.

2.3. Flame-Retardant and Smoke-Suppression Properties. As a critical factor that decides people's survival from fire incidents, smoke-suppression capability has drawn attention from researchers of flame retardants. It is also one of our focal points. The flammability of the samples was tested through UL-94 rating and LOI, with the results shown in Table 4. For 10 wt % Lig-P/EP, less improvement occurred in UL-94 tests, but the LOI value increased slightly. However, for 10 wt % Lig-M/EP, V-1 rating in the UL-94 test was achieved. Meanwhile, 6 wt % Lig-F/EP and 8 wt % Lig-F/EP both achieved V-1 rating and their LOI values increased to 33.3 and 34.2, respectively. For 10 wt % Lig-F/EP, the UL-94 grade reached V-0 and the LOI was as high as 34.3, which indicated that the appropriate N and P contents lead to a better flame-retardant effect. The excellent flame retardancy of our Lig/EP composites demonstrates our success in utilizing modified lignin as flame retardants. The actual UL-94 testing of 10% Lig-F/EP is shown in the video provided in the Supporting Information (Video 1).

Cone calorimeter tests were used to determine the heat release and smoke release of our composite samples. The heat release rate (HRR) and the total heat release (THR) curves of EP, 10%-Lig-P/EP, 10%-Lig-M/EP, and 10%-Lig-F/EP composites are shown in Figure 5. Table 5 includes detailed cone calorimeter data of EP and three Lig/EP composites. Among all of the samples, EP was most easily ignited and burnt, indicated by its shortest time to ignite (TTI) of 66 s and smallest residue (%) of 8.4%; TTI (s) and residue (%) exhibit significant increasing trends for the sample sequence from EP to Lig-P/EP, Lig-M/EP, and Lig-F/MP. In particular, TTI and residue values of Lig-F/EP are about 170 and 194% of the correspondent values of EP. The continuous increase of TTI and residue values indicates that the samples in the sequence become more difficult to ignite and have more charring residues after combustion, which is in agreement with the decrease of AMLR (Lig-F/EP is 61% of AMLR for EP). Meanwhile, PHRR and av-HRR values show a substantial decrease for the three Lig/EP composites. For lig-F/EP, they are 53 and 58% of the correspondent values of EP. The decreasing trend of PHRR and av-HRR indicates that the heat isolation capacity of the samples in the sequence is continuously enhanced. THR follows a decreasing trend from Lig-P/EP to Lig-M/EP and to Lig-F/EP. Lig-M and Lig-F composites show THR values smaller than that of EP. Notably, TSP values of all three Lig-/EP composites are less than 50% of that of EP; these represent strong evidence of excellent smoke-suppressing performances of the Lig/EP

https://dx.doi.org/10.1021/acsomega.0c05146
ACS Omega 2020, 5, 32084−32093

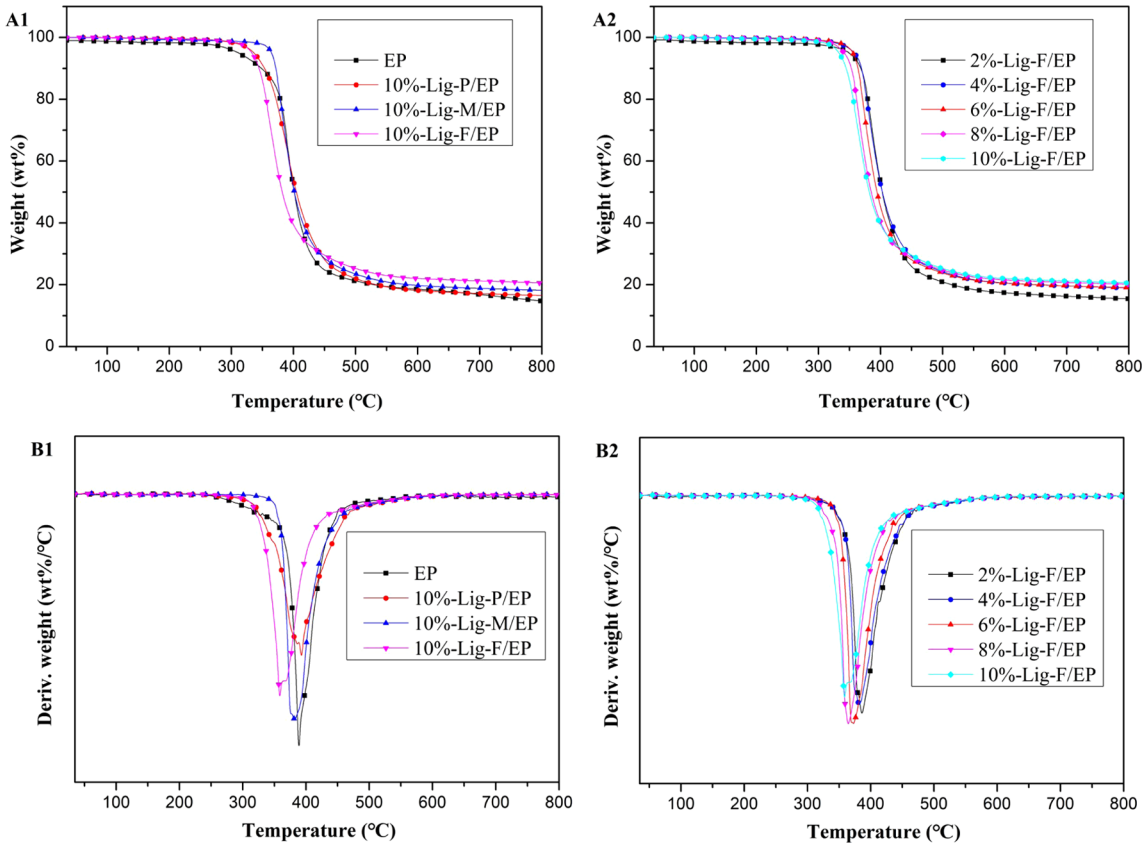

Figure 4. (A) TGA and (B) DTG curves: (1) EP, 10%-Lig-P/EP, 10%-Lig-M/EP, and 10%-Lig-F/EP and (2) 2%-Lig-F/EP, 4%-Lig-F/EP, 6%-Lig-F/EP, 8%-Lig-F/EP, and 10%-Lig-F/EP composites under a N_2 atmosphere at a heating rate of 20 °C/min.

Table 3. Initial Degradation Temperature (T_i), Maximum Weight Loss Temperature (T_{max}), and Carbon Residue (Char) of EP and Lig/EP Composites

sample	T_i (°C)	T_{max} (°C)	char (%, 800 °C)
EP	384	389	14.8
10%-Lig-P/EP	383	392	16.5
10%-Lig-M/EP	372	382	18.2
2%-Lig-F/EP	375	386	15.5
4%-Lig-F/EP	371	382	19.0
6% -Lig-F/EP	365	373	19.1
8%-Lig-F/EP	355	365	20.2
10%-Lig-F/EP	354	359	20.6

Table 4. UL-94 Level and LOI of EP and Lig/EP

sample	UL-94 level	LOI (%)
EP	no rating	23.3
10%-Lig-P/EP	no rating	24.7
10%-Lig-M/EP	V-1	31.6
2%-Lig-F/EP	no rating	26.2
4%-Lig-F/EP	no rating	28.5
6%-Lig-F/EP	V-1	33.3
8%-Lig-F/EP	V-1	34.2
10%-Lig-F/EP	V-0	34.3

composites. These trends indicate that modified lignin provides not only effective flame retardancy but is also environmentally friendly. Notably, the addition of Lig-F offers the best flame retardancy among all three Lig/EP composites.

Figure 5C,D further shows that the addition of Lig-P, Lig-M, and Lig-F can effectively reduce the smoke production (TSP) during combustion of corresponding Lig/EP composites. Lig-P reduces TSP by 63%. Lig-M/EP and Lig-F/EP reduce TSP values by 65 and 53%, respectively. Our results indicate that both Lig-M and Lig-F can improve flame-retardant and smoke-suppression effects. The slight difference in the smoke-suppression efficiency of Lig-M and Lig-F seems to be caused by their difference in element contents (N and P). This is consistent with the report that N and P contents in flame retardants can promote formation of stably expanded charring layers during combustion.[42]

2.4. Investigation of Char Residues. Figure 6 shows the morphology of each sample after combustion. The residues of EP and 10%-Lig-P/EP show the morphology of contraction, indicating lack of flame retardancy. For Lig-M/EP and Lig-F/EP, the residues present a morphology of expansion. This is because the charring layer expands due to formation of NH_3 from the thermal decomposition of N-containing groups.[43,44] Lig-M/EP, with a UL-94 rating of V-1, exhibits a much prominent expansion compared to Lig-F/EP, with a UL-94 rating of V-0. There are two reasons. Compared to Lig-F, the relatively higher N content in Lig-M leads to a larger amount of released NH_3 during the combustion; on the other hand, its slightly lower flame-retardant efficiency (compared to Lig-F) extends the combustion time, which further increases the amount of NH_3.

During combustion, nitrogen produces noncombustible gas and dilutes oxygen, which results in the expansion of the charring layer; when heated, phosphorus functional groups will decompose to form phosphoric acid or phosphate ester

https://dx.doi.org/10.1021/acsomega.0c05146
ACS Omega 2020, 5, 32084−32093

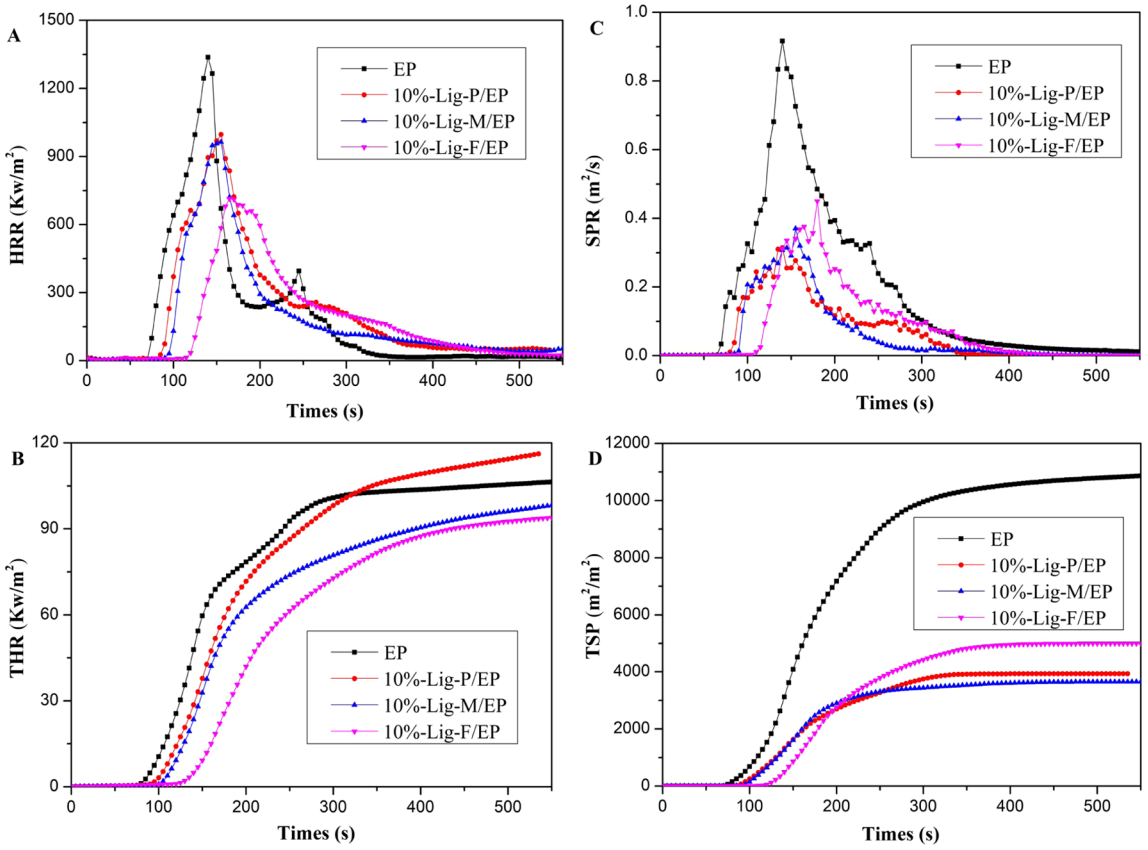

Figure 5. (A) Heat release rate, (B) total heat release curves, (C) smoke production rate, (D) and total smoke production rate of typical EP, 10%-Lig-P/EP, 10%-Lig-M/EP, and 10%-Lig-F/EP composites (100 × 100 × 3 mm^3) at a heat flux of 35 kW/m^2.

Table 5. Cone Calorimeter Data of EP and Lig/EP Composites

samples	TTI (s)	PHRR (kW/m^2)	av-HRR (kW/m^2)	THR (MJ/m^2)	residue (%)	AMLR (g/s)	TSP (m^2/m^2)
EP	66	1336.7	309.6	103.7	8.4	0.122	93.5
10%-Lig-P/EP	74	996.6	251.3	115.7	9.3	0.091	34.7
10%-Lig-M/EP	81	963.4	210.7	98.0	14.5	0.077	32.3
10%-Lig-F/EP	112	714.4	179.8	95.3	16.3	0.075	44.1

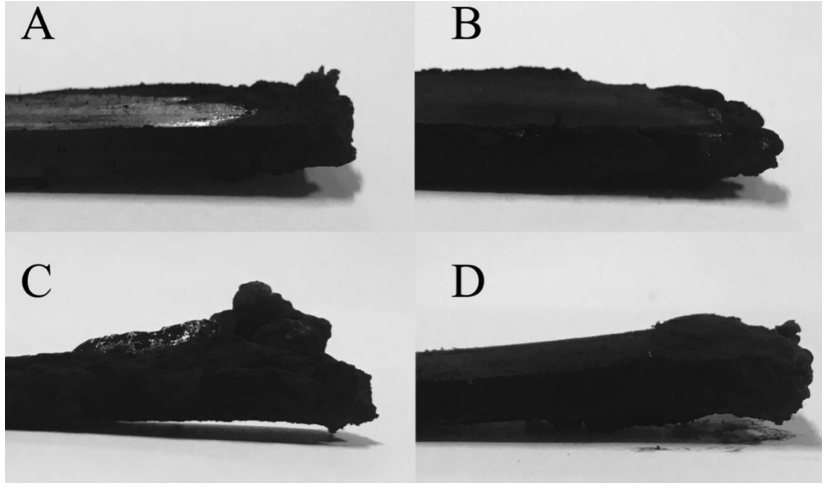

Figure 6. Digital photos of composites for (A) EP, (B) 10%-Lig-P/EP, (C) 10%-Lig-M/EP, and (D) 10%-Lig-F/EP after UL-94 testing.

compounds that prevent the spread of the flame. Lig-M and Lig-F can form a stable and continuous charring layer during combustion, which explains their excellent flame-retardant performance.

https://dx.doi.org/10.1021/acsomega.0c05146
ACS Omega 2020, 5, 32084−32093

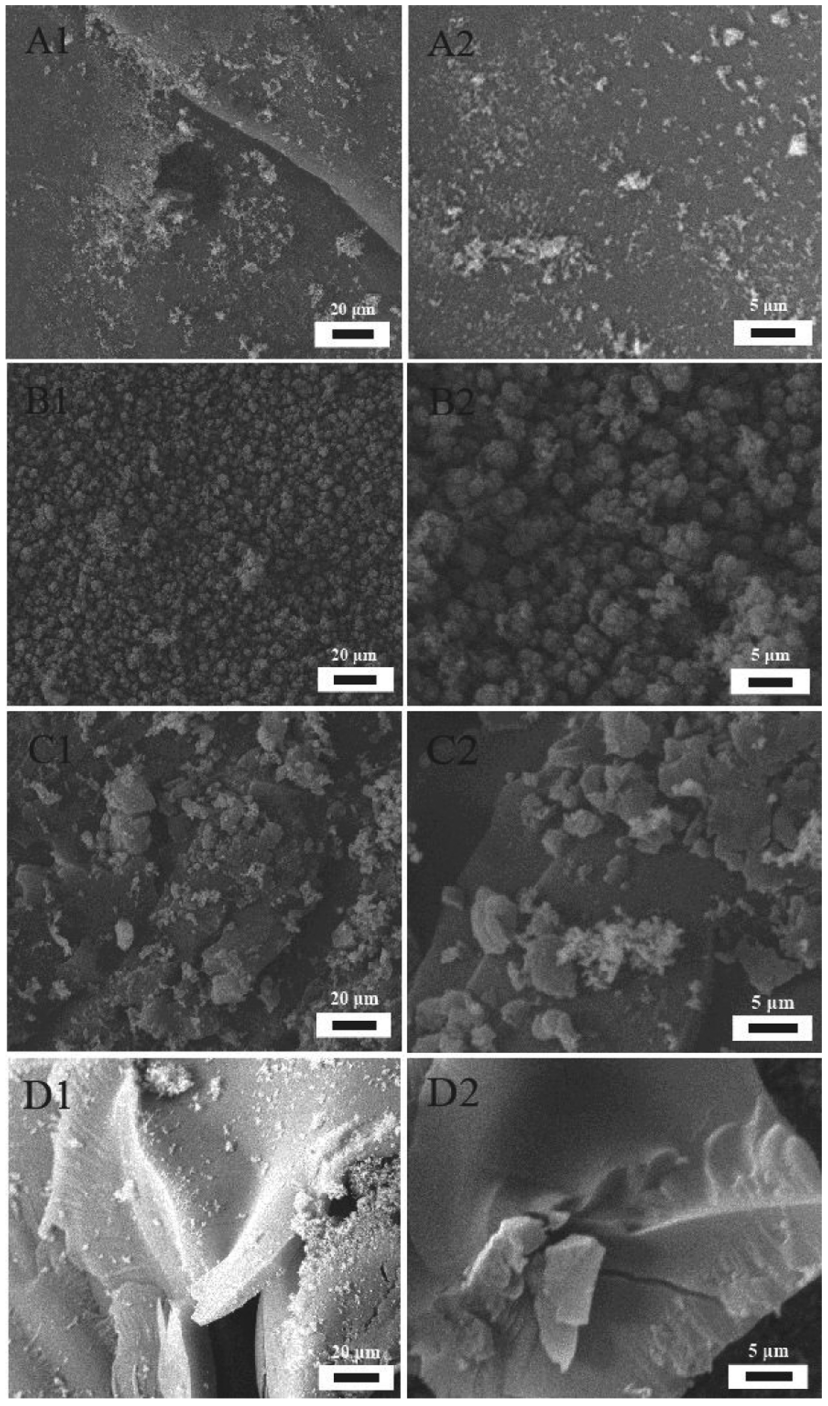

Figure 7. SEM images of the residue char: (A1, A2) for the EP composite; (B1, B2) for the 10%-Lig-P/EP composite; (C1, C2) for the 10%-Lig-M/EP composite; and (D1, D2) for 10%-Lig-F/EP composites.

SEM was used to obtain microscopic images of the residues after combustion. With two frame sizes, 5 μm (left) and 20 μm (right), Figure 7 contains images of the char residues, showing the morphology of residues after combustion of the composites. EP residues are tiny and crumby (A1, A2). Lig-P/EP residues are small, loose particles not aggregating to form a barrier (B1, B2). Lig-M/EP residues (C1, C2) reveal a charring layer made of particles aggregated into large blocks, which serve as a barrier to a certain degree (a limited improvement compared to EP and Lig-P/EP). Residuals of Lig-F/EP show formation of an extended and intact charring layer, a most effective structure in insulating heat and air during combustion (D1, D2). This explains why Lig-F is the most efficient flame retardant. From A through D in Figure 7, a clear trend was observed: the charring layer becomes larger and more extended, which explains the differences in flame-retardant properties for the four composites.

Graphitization degrees of the char residues were explored by Raman spectroscopy. Figure 8 shows the D bands and G bands of the four composites. The G band is related to the vibrations of the sp^2-hybridized carbon atoms, and the D band is related to the vibrations of the disordered terminal carbon atoms.[45] The intensity ratio of the D band and the G band, I_D/I_G, is inversely proportional to the graphitization degree of the

https://dx.doi.org/10.1021/acsomega.0c05146
ACS Omega 2020, 5, 32084−32093

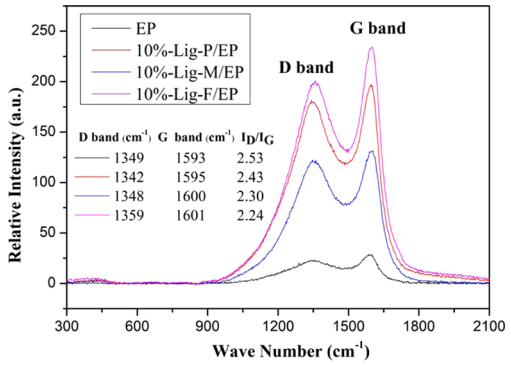

Figure 8. Raman spectra of the carbon residue for (a) EP, (b) 10%-Lig-P/EP, (c) 10%-Lig-M/EP, and (d) 10%-Lig-F/EP composites.

carbon residue. The I_D/I_G ratio of 10 wt % Lig-F/EP is 2.24 (the lowest), indicating that Lig-F/EP has the highest level of graphitization (best charring performance). The degree of graphitization of the charring layer has an increasing trend, following the order of lignin modification presented previously, as shown in Figure 8.

It is noticeable in the Raman spectra that both D and G bands show a slight blue shift from Lig-P/EP to Lig-M/EP, and to Lig-F/EP. This is related to P bonding with C in the residuals: an increase of the P content leads to more blue shift.[29] This is consistent with the fact that we have added more P in Lig-F than in Lig-M, and no P is added in Lig-P.

2.5. Mechanisms: Flame Retardancy and Beyond. The improvements of flame-retardant properties of the Lig/EP systems can be explained by several mechanisms working coherently in both the condensed phase and gas phase. In the condensed phase, decomposition products of DOPO in the modified lignin play an important role, including phosphoric acid, pyrophosphoric acid, and polyphosphoric acid. These acids promote dehydration reactions of lignin and EP[46,47] to produce carbonaceous materials, which forms a charring layer, which is capable of reducing heat transfer, isolating oxygen, and preventing further burning of degraded polymer particles. Besides, lignin itself has excellent charring capacity during the combustion process. Its benzene ring and phenol structure help enhance the compactness of the charring layer and increase its thermal barrier property. In the gas phase, nonflammable gases, formed from decomposition of piperazine during the combustion, will dilute the concentration of O_2 in the combustion zone, delaying the combustion process and reducing heat release. In addition, the phosphorus-based radicals formed by the decomposition of DOPO will quench active radicals and inhibit combustion.[48,49] The synergistic effects in the two phases lead to the excellent flame retardance of Lig-M and even better performance of Lig-F. The smoke suppression is also related to formation of the charring layer. In general, a larger and denser charring layer prevents small, light particulate matters from leaving the composite and forming smoke.

3. CONCLUSIONS

We developed a novel method of synthesizing flame retardants with lignin modified with N and P. The three lignin-based EP composites Lig-P, Lig-M, and Lig-F were characterized and tested for their flame-retardant and smoke-suppression properties. Our results show that these flame retardants are not only effective but also environmentally friendly. Two of the composites achieved UL-test grading of V-1 and V-0. In the meantime, our flame retardants also exhibit excellent smoke-suppression performance.

We proposed the flame-retarding mechanisms considering condensed and gas phases, and we believe that the synergistic

Scheme 1. Synthetic Route of Modified Lignin (Lig-M and Lig-F)

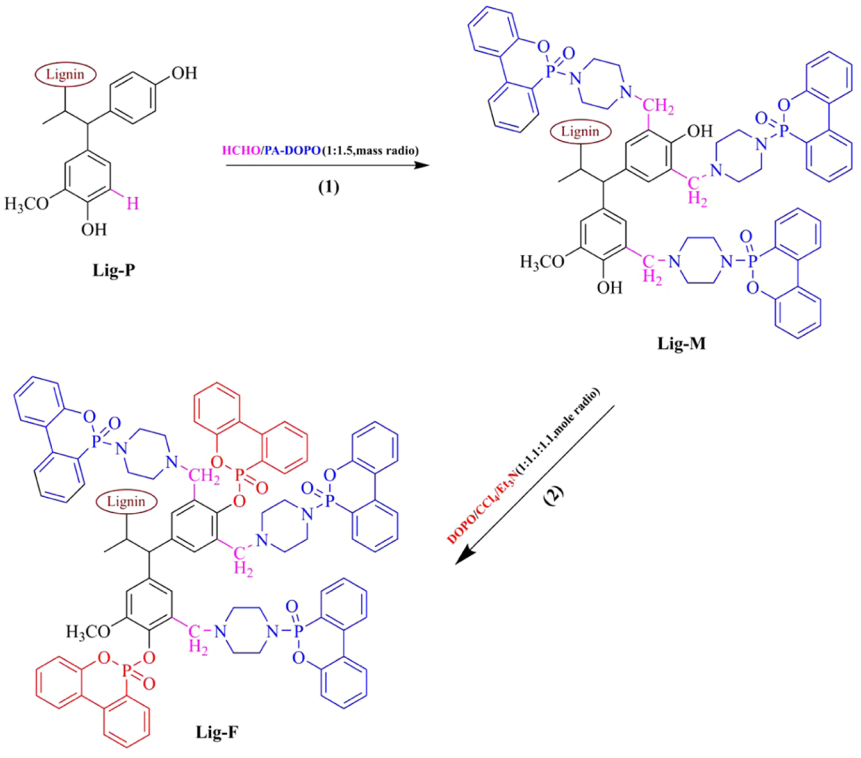

https://dx.doi.org/10.1021/acsomega.0c05146
ACS Omega 2020, 5, 32084−32093

effect of nitrogen and phosphorus in lignin was responsible for the improvement of fire-resistant properties. Further, formation of a larger and denser charring layer helps in improving smoke suppression. This work provides an effective and environmentally friendly means of achieving flame retardancy and smoke suppression using modified lignin.

4. METHODS AND MATERIALS

4.1. Materials. Epoxy resin (commercial name: E51) was purchased from Wuxi Bluestar Resin Factory. Lignin (enzymatic hydrolysis lignin, 4.1 mmol/g OH, with M_w and M_n of 3259 and 1385 g/mol) was bought from Shandong Longli Biotechnology Co., Ltd., Shandong, China. Other chemical agents such as phenol, terephthalaldehyde, 4,4′-diaminodiphenylmethane (DDM), DOPO, PA, dimethylformamide (DMF), dichloromethane (CH_2Cl_2), carbon tetrachloride (CCl_4), sodium hydroxide (NaOH), triethylamine (Et_3N), 37% formaldehyde (HCHO), and ethanol were purchased from Macklin, China.

4.2. Preparation of Lig-M. Lig-P (10 g) and the intermediate PA−DOPO (27 g) (see Scheme S2 in the Supporting Information) were dissolved in 200 mL of DMF. Formaldehyde solution (18 g, 37%) was added dropwise to the DMF solution at 75 °C, and the reaction mixture was refluxed for 3 h. Upon completion of the reaction, excess distilled water was added to obtain the precipitate, which was washed three times by ethanol and dried under vacuum at 80 °C for 12 h. The product (yield: 42.0%) was labeled Lig-M.

4.3. Preparation of Lig-F. Lig-M (2.7 g), Et_3N (2.72 g), and DOPO (5.83 g) were dissolved in DMF (50 mL). To the mixture, CCl_4 (4.13 g) was added dropwise at 0 °C under a N_2 atmosphere, allowing the reaction to continue for 10 h at 25 °C. The precipitate obtained was washed in the same way as described in Section 2.2. The product (yield: 46.9%) was labeled Lig-F, as shown in Scheme 1.

4.4. Composite Fabrication. The lignin-based flame retardant was added to 20 g of EP and stirred for 1 h; then, 4 g of DDM was added and stirred for another 1 h. The reaction mixture was poured into a grinding tool and cured at 100 °C for 2 h, and further cured for 2 h at 150 °C. The epoxy composite was obtained after curing and demolding. The formulations of all EP composites are listed in Table 6.

4.5. Characterization. FTIR spectra were obtained with a Bruker VERTEX 80V FT-IR spectrometer. Elemental analysis (EA) was carried out on a 2400 II (PE, America) elemental analyzer. X-ray photoelectron spectroscopy (XPS) was performed on a Shimadzu AXIS Ultra DLD spectrometer (settings: energy analyzer fixed at 0.48 eV, power at 150 W, and beam spot at 300 × 700 μm^2). Thermogravimetric analysis (TGA) was conducted on a NETZSCH (Germany) TG 209F1 instrument.

An EP composite sample of 8.0 mg was heated to 800 °C at a heating rate of 20 °C/min under a N_2 atmosphere. The combustion performance of each Lig/EP composite sample with a size of 100 × 10 × 3 mm^3 was examined on the CFZ-2 Horizontal-Vertical Burning Tester (Jiangsu Institute of Chemical Industry), to obtain the UL-94 rating (based on ASTM D3801-19 UL-94 standard). The limiting oxygen index (LOI) tests of the Lig/EP composite samples were performed on an HC-2 LOI instrument (Jiangsu Institute of Chemical Industry), according to the ASTM D2863 standard. Flame-retardant properties of the samples (100 × 100 × 3 mm^3) were tested at another facility via a cone calorimeter (FTT, U.K.), using the ISO 5660 protocol, except that samples were tested only once rather than in triplicate as per the ISO 5660 methodology. Samples were tested with a metal frame and aluminum foil backing at a heat flux of 35 kW/m^2. Since samples were tested only once, the results of the test can be referenced. SEM images were obtained using a Quanta 200 (FEI, America) at an accelerating voltage of 5 kV. Raman spectroscopy was performed on a DXR532 Raman spectrometer (Thermo Fisher Scientific, America) at 780 nm.

Table 6. Formulations of EP Composites

sample	EP (wt %)	DDM (wt %)	Lig-P (wt %)	Lig-M (wt %)	Lig-F (wt %)
EP	83.3	16.7	0	0	0
10%-Lig-P/EP	75.0	15.0	10	0	0
10%-Lig-M/EP	75.0	15.0	0	10	0
2%-Lig-F/EP	81.7	16.3	0	0	2
4%-Lig-F/EP	80.0	16.0	0	0	4
6%-Lig-F/EP	78.3	25.7	0	0	6
8%-Lig-F/EP	76.5	15.5	0	0	8
10%-Lig-F/EP	75.0	15	0	0	10

■ ASSOCIATED CONTENT

Supporting Information

The Supporting Information is available free of charge at https://pubs.acs.org/doi/10.1021/acsomega.0c05146.

Video of UL-94 testing with the 10%-Lig-F/EP composite (MP4)

Preparation of PA−DOPO; preparation of Lig-P; characterization of PA−DOPO; characterization of pretreated lignin (Lig-P); effective heat of combustion; and analysis of mechanical properties of Lig-F (PDF)

■ AUTHOR INFORMATION

Corresponding Author

Zhenyang Luo − *College of Science and Institute of Polymer Materials, Nanjing Forestry University, Nanjing 210037, P. R. China;* orcid.org/0000-0001-5063-2856; Email: luozhenyang@njfu.edu.cn

Authors

Peng Dai − *College of Science, Nanjing Forestry University, Nanjing 210037, P. R. China*

Mengke Liang − *College of Science, Nanjing Forestry University, Nanjing 210037, P. R. China*

Xiaofeng Ma − *College of Science and Institute of Polymer Materials, Nanjing Forestry University, Nanjing 210037, P. R. China*

Yanlong Luo − *College of Science and Institute of Polymer Materials, Nanjing Forestry University, Nanjing 210037, P. R. China;* orcid.org/0000-0002-7765-7911

Ming He − *College of Science and Institute of Polymer Materials, Nanjing Forestry University, Nanjing 210037, P. R. China;* orcid.org/0000-0002-9315-0424

Xiaoli Gu − *College of Chemical Engineering, Nanjing Forestry University, Nanjing 210037, P. R. China*

Qun Gu − *Department of Chemistry, Edinboro University of Pennsylvania, Edinboro, Pennsylvania 16444, United States*

https://dx.doi.org/10.1021/acsomega.0c05146
ACS Omega 2020, 5, 32084−32093

Imtiaz Hussain − *College of Science, Nanjing Forestry University, Nanjing 210037, P. R. China*

Complete contact information is available at: https://pubs.acs.org/10.1021/acsomega.0c05146

Author Contributions

[⊥]P.D. and M.L. contributed equally to this work.

Notes

The authors declare no competing financial interest.

■ ACKNOWLEDGMENTS

This work was supported by the National Natural Science Foundation of China (21774059). This work was also supported by a project funded by the Priority Academic Program Development of Jiangsu Higher Education Institutions (PAPD). The authors are grateful for the nuclear magnetic spectrometer provided by the Advanced Analysis and Testing Center of Nanjing Forestry University, and the guidance of Dr. Shilong Yang.

■ REFERENCES

(1) Jin, F.; Li, X.; Park, S. Synthesis and application of epoxy resins: A review. *J. Ind. Eng. Chem.* **2015**, *29*, 1−11.

(2) Hu, Y.; Yuan, B.; Cheng, F.; Hu, X. NaOH etching and resin precoating treatments for stronger adhesive bonding between CFRP and aluminium alloy. *Composites, Part B* **2019**, *178*, No. 107478.

(3) Castro-Aguirre, E.; Iñiguez-Franco, F.; Samsudin, H.; Fang, X.; Auras, R. Poly(lactic acid)—Mass production, processing, industrial applications, and end of life. *Adv. Drug Delivery Rev.* **2016**, *107*, 333−366.

(4) Wang, S.; Ma, S.; Xu, C.; Liu, Y.; Dai, J.; Wang, Z.; Liu, X.; Chen, J.; Shen, X.; Wei, J.; Zhu, J. Vanillin-Derived High-Performance Flame Retardant Epoxy Resins: Facile Synthesis and Properties. *Macromolecules* **2017**, *50*, 1892−1901.

(5) Wu, C.; Wang, X.; Zhang, J.; Cheng, J.; Shi, L. Microencapsulation and Surface Functionalization of Ammonium Polyphosphate via In-Situ Polymerization and Thiol−Ene Photograted Reaction for Application in Flame-Retardant Natural Rubber. *Ind. Eng. Chem. Res.* **2019**, *58*, 17346−17358.

(6) Li, X.; Zhang, F.; Jian, R.; Ai, Y.; Ma, J.; Hui, G.; Wang, D. Influence of eco-friendly calcium gluconate on the intumescent flame-retardant epoxy resin: Flame retardancy, smoke suppression and mechanical properties. *Composites, Part B* **2019**, *176*, No. 107200.

(7) Lu, S.; Hamerton, I. Recent developments in the chemistry of halogen-free flame retardant polymers. *Prog. Polym. Sci.* **2002**, *27*, 1661−1712.

(8) Wang, X.; Hu, Y.; Song, L.; Xing, W.; Lu, H.; Lv, P.; Jie, G. Effect of a triazine ring-containing charring agent on fire retardancy and thermal degradation of intumescent flame retardant epoxy resins. *Polym. Adv. Technol.* **2011**, *22*, 2480−2487.

(9) Cheng, X.; Guan, J.; Yang, X.; Tang, R.; Yao, F. A bio-resourced phytic acid/chitosan polyelectrolyte complex for the flame retardant treatment of wool fabric. *J. Cleaner Prod.* **2019**, *223*, 342−349.

(10) Zhang, X.; Cao, J.; Yang, Y.; Wu, X.; Zheng, Z.; Zhang, X. Flame-retardant, highly sensitive strain sensors enabled by renewable phytic acid-doped biotemplate synthesis and spirally structure design. *Chem. Eng. J.* **2019**, *374*, 730−737.

(11) Daniel, Y. G.; Howell, B. A. Flame retardant properties of isosorbide bis-phosphorus esters. *Polym. Degrad. Stab.* **2017**, *140*, 25−31.

(12) Zhang, L.; Zhang, M.; Hu, L.; Zhou, Y. Synthesis of rigid polyurethane foams with castor oil-based flame retardant polyols. *Ind. Crops Prod.* **2014**, *52*, 380−388.

(13) Zheng, C.; Wen, S.; Teng, Z.; Ye, C.; Chen, Q.; Zhuang, Y.; Zhang, G.; Cai, J.; Fei, P. Formation of $H_2Ti_2O_5{\cdot}H_2O$ nanotube-based hybrid coating on bamboo fibre materials through layer-by-layer self-assembly method for an improved flame retardant performance. *Cellulose* **2019**, *26*, 2729−2741.

(14) Amarnath, N.; Appavoo, D.; Lochab, B. Eco-Friendly Halogen-Free Flame Retardant Cardanol Polyphosphazene Polybenzoxazine Networks. *ACS Sustainable Chem. Eng.* **2018**, *6*, 389−402.

(15) Zhang, J.; Yue, L.; Kong, Q.; Liu, Z.; Zhou, X.; Zhang, C.; Xu, Q.; Zhang, B.; Ding, G.; Qin, B.; Duan, Y.; Wang, Q.; Yao, J.; Cui, G.; Chen, L. Sustainable, heat-resistant and flame-retardant cellulose-based composite separator for high-performance lithium ion battery. *Sci. Rep.* **2015**, *4*, No. 3935.

(16) Feng, J.; Sun, Y.; Song, P.; Lei, W.; Wu, Q.; Liu, L.; Yu, Y.; Wang, H. Fire-Resistant, Strong, and Green Polymer Nanocomposites Based on Poly(lactic acid) and Core-Shell Nanofibrous Flame Retardants. *ACS Sustainable Chem. Eng.* **2017**, *5*, 7894−7904.

(17) Chollet, B.; Lopez-Cuesta, J.; Laoutid, F.; Ferry, L. Lignin Nanoparticles as A Promising Way for Enhancing Lignin Flame Retardant Effect in Polylactide. *Materials* **2019**, *12*, 2132.

(18) Li, P.; Sirviö, J. A.; Hong, S.; Ämmälä, A.; Liimatainen, H. Preparation of flame-retardant lignin-containing wood nanofibers using a high-consistency mechano-chemical pretreatment. *Chem. Eng. J.* **2019**, *375*, No. 122050.

(19) Kubo, S.; Kadla, J. F. Poly(Ethylene Oxide)/Organosolv Lignin Blends: Relationship between Thermal Properties, Chemical Structure, and Blend Behavior. *Macromolecules* **2004**, *37*, 6904−6911.

(20) Brebu, M.; Tamminen, T.; Spiridon, I. Thermal degradation of various lignins by TG-MS/FTIR and Py-GC-MS. *J. Anal. Appl. Pyrolysis* **2013**, *104*, 531−539.

(21) Brodin, I.; Sjöholm, E.; Gellerstedt, G. The behavior of kraft lignin during thermal treatment. *J. Anal. Appl. Pyrolysis* **2010**, *87*, 70−77.

(22) Xing, W.; Yuan, H.; Zhang, P.; Yang, H.; Song, L.; Hu, Y. Functionalized lignin for halogen-free flame retardant rigid polyurethane foam: preparation, thermal stability, fire performance and mechanical properties. *J. Polym. Res.* **2013**, *20*, 234.

(23) De Chirico, A.; Armanini, M.; Chini, P.; Cioccolo, G.; Provasoli, F.; Audisio, G. Flame retardants for polypropylene based on lignin. *Polym. Degrad. Stab.* **2003**, *79*, 139−145.

(24) Zhang, R.; Xiao, X.; Tai, Q.; Huang, H.; Yang, J.; Hu, Y. Preparation of lignin−silica hybrids and its application in intumescent flame-retardant poly(lactic acid) system. *High Perform. Polym.* **2012**, *24*, 738−746.

(25) Li, J.; Yan, Q.; Zhang, X.; Zhang, J.; Cai, Z. Efficient Conversion of Lignin Waste to High Value Bio-Graphene Oxide Nanomaterials. *Polymers* **2019**, *11*, 623.

(26) Song, P.; Cao, Z.; Fu, S.; Fang, Z.; Wu, Q.; Ye, J. Thermal degradation and flame retardancy properties of ABS/lignin: Effects of lignin content and reactive compatibilization. *Thermochim. Acta* **2011**, *518*, 59−65.

(27) Cholake, S. T.; Rajarao, R.; Henderson, P.; Rajagopal, R. R.; Sahajwalla, V. Composite panels obtained from automotive waste plastics and agricultural macadamia shell waste. *J. Cleaner Prod.* **2017**, *151*, 163−171.

(28) Liu, L.; Huang, G.; Song, P.; Yu, Y.; Fu, S. Converting Industrial Alkali Lignin to Biobased Functional Additives for Improving Fire Behavior and Smoke Suppression of Polybutylene Succinate. *ACS Sustainable Chem. Eng.* **2016**, *4*, 4732−4742.

(29) Costes, L.; Laoutid, F.; Aguedo, M.; Richel, A.; Brohez, S.; Delvosalle, C.; Dubois, P. Phosphorus and nitrogen derivatization as efficient route for improvement of lignin flame retardant action in PLA. *Eur. Polym. J.* **2016**, *84*, 652−667.

(30) Wu, W.; He, H.; Liu, T.; Wei, R.; Cao, X.; Sun, Q.; Venkatesh, S.; Yuen, R. K. K.; Roy, V. A. L.; Li, R. K. Y. Synergetic enhancement on flame retardancy by melamine phosphate modified lignin in rice husk ash filled P34HB biocomposites. *Compos. Sci. Technol.* **2018**, *168*, 246−254.

(31) Liu, L.; Qian, M.; Song, P. A.; Huang, G.; Yu, Y.; Fu, S. Fabrication of Green Lignin-based Flame Retardants for Enhancing the Thermal and Fire Retardancy Properties of Polypropylene/Wood Composites. *ACS Sustainable Chem. Eng.* **2016**, *4*, 2422−2431.

(32) Zhou, S.; Tao, R.; Dai, P.; Luo, Z.; He, M. Two-step fabrication of lignin-based flame retardant for enhancing the thermal and fire retardancy properties of epoxy resin composites. *Polym. Compos.* **2020**, *41*, 2025−2035.
(33) Hu, W.; Zhang, Y.; Qi, Y.; Wang, H.; Liu, B.; Zhao, Q.; Zhang, J.; Duan, J.; Zhang, L.; Sun, Z.; Liu, B. Improved Mechanical Properties and Flame Retardancy of Wood/PLA All-Degradable Biocomposites with Novel Lignin-Based Flame Retardant and TGIC. *Macromol. Mater. Eng.* **2020**, *305*, No. 1900840.
(34) Xie, W.; Tang, D.; Liu, S.; Zhao, J. Facile synthesis of bio-based phosphorus-containing epoxy resins with excellent flame resistance. *Polym. Test.* **2020**, *86*, No. 106466.
(35) Guo, W.; Zhao, Y.; Wang, X.; Cai, W.; Wang, J.; Song, L.; Hu, Y. Multifunctional epoxy composites with highly flame retardant and effective electromagnetic interference shielding performances. *Composites, Part B* **2020**, *192*, No. 107990.
(36) Liu, C.; Yao, Q. Design and Synthesis of Efficient Phosphorus Flame Retardant for Polycarbonate. *Ind. Eng. Chem. Res.* **2017**, *56*, 8789−8796.
(37) Neisius, N. M.; Lutz, M.; Rentsch, D.; Hemberger, P.; Gaan, S. Synthesis of DOPO-Based Phosphonamidates and their Thermal Properties. *Ind. Eng. Chem. Res.* **2014**, *53*, 2889−2896.
(38) Wagner, S.; Rakotomalala, M.; Chesneau, F.; Zevaco, T.; Doering, M. Spectral Assignment of Phenanthrene Derivatives Based on 6H-Dibenzo[C,E][1,2] Oxaphosphinine 6-Oxide by NMR and Quantum Chemical Calculations. *Phosphorus, Sulfur Silicon Relat. Elem.* **2012**, *187*, 781−798.
(39) Yu, Y.; Fu, S.; Song, P. A.; Luo, X.; Jin, Y.; Lu, F.; Wu, Q.; Ye, J. Functionalized lignin by grafting phosphorus-nitrogen improves the thermal stability and flame retardancy of polypropylene. *Polym. Degrad. Stab.* **2012**, *97*, 541−546.
(40) Huo, S.; Yang, S.; Wang, J.; Cheng, J.; Zhang, Q.; Hu, Y.; Ding, G.; Zhang, Q.; Song, P. A liquid phosphorus-containing imidazole derivative as flame-retardant curing agent for epoxy resin with enhanced thermal latency, mechanical, and flame-retardant performances. *J. Hazard. Mater.* **2020**, *386*, No. 121984.
(41) Fang, F.; Huo, S.; Shen, H.; Ran, S.; Wang, H.; Song, P.; Fang, Z. A bio-based ionic complex with different oxidation states of phosphorus for reducing flammability and smoke release of epoxy resins. *Compos. Commun.* **2020**, *17*, 104−108.
(42) Shao, Z.; Deng, C.; Tan, Y.; Chen, M.; Chen, L.; Wang, Y. An Efficient Mono-Component Polymeric Intumescent Flame Retardant for Polypropylene: Preparation and Application. *ACS Appl. Mater. Interfaces* **2014**, *6*, 7363−7370.
(43) Xue, Y.; Feng, J.; Huo, S.; Song, P.; Yu, B.; Liu, L.; Wang, H. Polyphosphoramide-intercalated MXene for simultaneously enhancing thermal stability, flame retardancy and mechanical properties of polylactide. *Chem. Eng. J.* **2020**, *397*, No. 125336.
(44) Yang, H.; Yu, B.; Xu, X.; Bourbigot, S.; Wang, H.; Song, P. Lignin-derived bio-based flame retardants toward high-performance sustainable polymeric materials. *Green Chem.* **2020**, *22*, 2129−2161.
(45) Tang, T.; Chen, X.; Meng, X.; Chen, H.; Ding, Y. Synthesis of Multiwalled Carbon Nanotubes by Catalytic Combustion of Polypropylene. *Angew. Chem., Int. Ed.* **2005**, *44*, 1517−1520.
(46) Qian, L.; Qiu, Y.; Wang, J.; Xi, W. High-performance flame retardancy by char-cage hindering and free radical quenching effects in epoxy thermosets. *Polymer* **2015**, *68*, 262−269.
(47) Liu, X.; Liu, B.; Luo, X.; Guo, D.; Zhong, H.; Chen, L.; Wang, Y. A novel phosphorus-containing semi-aromatic polyester toward flame retardancy and enhanced mechanical properties of epoxy resin. *Chem. Eng. J.* **2020**, *380*, No. 122471.
(48) Duan, H.; Chen, Y.; Ji, S.; Hu, R.; Ma, H. A novel phosphorus/nitrogen-containing polycarboxylic acid endowing epoxy resin with excellent flame retardance and mechanical properties. *Chem. Eng. J.* **2019**, *375*, No. 121916.
(49) Zhang, J.; Mi, X.; Chen, S.; Xu, Z.; Zhang, D.; Miao, M.; Wang, J. A bio-based hyperbranched flame retardant for epoxy resins. *Chem. Eng. J.* **2020**, *381*, No. 122719.

https://dx.doi.org/10.1021/acsomega.0c05146
ACS Omega 2020, 5, 32084−32093